Available online at www.sciencedirect.com
ScienceDirect
Journal of Process Control 18 (2008) 347–360
JOURNAL OF PROCESS CONTROL
www.elsevier.com/locate/jprocont

A continuous stirred tank heater simulation model with applications

Nina F. Thornhill [a,*], Sachin C. Patwardhan [b], Sirish L. Shah [c]

[a] Centre for Process Systems Engineering, Department of Chemical Engineering, Imperial College London, London SW7 2AZ, UK
[b] Department of Chemical Engineering, I.I.T. Bombay, Powai, Mumbai 400 076, India
[c] Department of Chemical and Materials Engineering, University of Alberta, Edmonton, Canada T6G 2G6

Received 18 December 2006; received in revised form 2 July 2007; accepted 11 July 2007

Abstract

This article presents a first principles simulation of a continuous stirred tank heater pilot plant at the University of Alberta. The model has heat and volumetric balances, and a very realistic feature is that instrument, actuator and process non-linearities have been carefully measured, for instance to take account of the volume occupied by heating coils in the tank. Experimental data from step testing and recordings of real disturbances are presented. The model in Simulink and the experimental data are available electronically, and some suggestions are given for their application in education, system identification, fault detection and diagnosis.

Keywords: Benchmark simulation; Disturbance; Experimental validation; First-principles model; Hybrid model; Performance analysis; System identification

1. Introduction

Process simulations are of value to university teachers and academic researchers because they allow comparisons and demonstrations of the merits of different approaches in areas such as control design, system identification and fault diagnosis.

This paper has an educational purpose. It describes a simulation of an experimental continuous stirred tank heater (CSTH) pilot plant. Volumetric and heat balance equations are presented along with algebraic equations derived from experimental data for calibration of sensors and actuators and unknown quantities such heat transfer through the heating coils. Many of these relationships have non-linearities, and hard constraints such as the tank being full are also captured. A valuable feature is that the model uses measured, not simulated, noise and disturbances and therefore provides a realistic platform for data-driven identification and fault detection. Code and data for the simulation presented in this article are available from the CSTH simulation website [38]. The model has been implemented in the Simulink simulation platform with a view to easy accessibility by students and researchers.

The next section of the paper reviews benchmark models from the process systems literature and places the CSTH model in context. Section 3 presents the pilot plant, relevant equations and the calibrations. Section 4 describes implementation of the model in the Simulink simulation platform. Section 5 presents experimental data for model validation while Section 6 shows the time trends of process and measurement disturbances captured from the experimental plant. All of these data sets are available at the CSTH web site. The model is then explored mathematically to give a linearized state-space representation at the operating point and also an input–output transfer function matrix representation. Finally, Section 8 suggests some applications for the simulation and presents a challenge in the form of a system identification problem.

* Corresponding author. Tel.: +44 0 20 7594 6622; fax: +44 0 20 7594 6606.
E-mail address: n.thornhill@imperial.ac.uk (N.F. Thornhill).

0959-1524/$ - see front matter © 2007 Elsevier Ltd. All rights reserved.
doi:10.1016/j.jprocont.2007.07.006

2. Background and context

2.1. Introduction

Process simulations in the public domain have been used in education and academic research for many years to compare the performance and applicability of methods for control, identification and diagnosis. Broadly speaking, the simulations fall into two categories: (i) models in which the dynamics are captured through first principles, and (ii) linear models presented as transfer functions or in state-space form. Also available are detailed models for individual components of a process such as control valves and rotating machinery. Commercial training simulators are a further important category of process simulation. The following sections review the literature and place the CSTH simulation in the context of other work.

2.2. First principles models

A very widely used model is the classic continuous stirred tank reactor simulation with Van de Vusse reaction kinetics [39]. It appears in text books [26,10] and has been used for demonstration of control schemes and fault diagnosis. The reaction equations are non-linear because they include the bilinear products of flow rates, composition and temperature as well as the temperature dependence of reaction rate [26]. Other authors have made realistic additions such as the dynamics of a reactor with a cooling jacket [31,32].

At the time of writing, more than 150 articles in the Science Citation index are using the Tennessee Eastman challenge problem [9]. This simulation represents a complete process comprising a reactor and several separation columns and heat exchangers. The process presents significant plant-wide multivariable control challenges and the authors also provided simulations of process faults. A baseline control system was reported by [24] and the simulation has been widely used for demonstration of advanced control schemes (e.g. [23,30,22,20,40]), and for testing of fault detection and diagnosis schemes, both data driven and model-based [19,12,5,14–16,34]. The original code was written in Fortran, while [29] has made an implementation in Simulink available to other researchers.

Other first principles models from the literature are:

- The vinyl acetate process [4];
- The reactor/regenerator section of a Model IV fluid catalytic cracking unit [25];
- Emulsion polymerization with population and particle balance [11];
- The ALSTOM gasifier that produces gas from carbon-based feedstock [8,7];
- Non-linear distillation model [35]. Matlab code is available for this simulation [36].

2.3. Linear dynamic models

The non-linear distillation model paper of [35] offered transfer function models linearized at different operating points as well as the first principles model.

Models expressed in the form of a transfer function matrix are helpful for demonstrating multivariable problems where interactions are the key issue. Their clear capture of these effects also gives them value for teaching purposes. For instance, [33] use the Wood–Berry two-by-two transfer function model of a pilot-scale distillation [42]. The model relates plant inputs (reflux rate and steam flow rate) to outputs (top and bottom product compositions). It is expressed as transfer functions in the form of first order lags plus time delays (FOPTD). [21] used the Wood–Berry model to demonstrate performance monitoring of a model predictive controller.

The Shell challenge problem [28] is a transfer function representation of an industrial debutanizer. Again, each transfer function is a first order lag with delay where some of the delays are very long, giving a considerable challenge for multivariable control. The paper by [3] concerned worst-case bounds and statistical uncertainty in the evaluation of the Relative Gain Array. It presented results from several transfer function benchmark models including a simplified model for the Shell challenge problem and a three-by-three model for a pilot scale distillation column which originated with [27].

State-space benchmarks are used for the testing of model reduction algorithms in which the aim is to derive a smaller representation with many fewer states which has almost the same dynamic input–output behaviour as the original problem. The SLICOT collection [37] created as part of the European Union's BRITE-EURAM III NICONET programme gives some huge state-space models as challenges for this purpose and the Oberwolfach model reduction benchmark collection [18] has similar uses.

2.4. Hybrid and data-based models

An issue with the use of simulations for applications in fault diagnosis and robust control can be that noise and disturbances are difficult to model accurately. There is a tendency to model these as filtered or integrated Gaussian random noise or as piecewise linear disturbances, but in many case such simple signals fail to capture real effects. For instance, time trends of instruments measuring the output of a non-linear system typically have a non-Gaussian distribution and a spectrum characterized by phase coupling. Real data captured from processes provide more realistic tests than simulated data.

[41] provided benchmark data for a non-linear dynamic model identification challenge problem. The data are from a laboratory surge tank which generated non-linear input–output data for the comparison of non-linear modeling methods. A specific issue was that models should be robust to noise in the identification data.

The approach taken by [17] combined measurements from a real process with a simulated exothermic reaction. The process is a tank that behaves as if an exothermic reaction is taking place. There are no real reactants and instead the reaction is simulated. The reactant feed rate in the model is set to the measured cold water feed rate, while directly injected steam provides the heat released by the simulated reaction. The partially simulated reactor provides a platform for testing of control strategies under realistic conditions of process constrains, measurement noise, quanitized measurements and sampled data control.

2.5. Equipment models

Published models are available for components and items of equipment. The DAMADICS simulation [2] provides a benchmark challenge in identification of control valve faults. It comprises a Simulink model of a specific valve in a sugar refinery with properties such as friction together with data from the refinery that capture normal running and several valve faults. [6] created an empirical model of a valve with parameters that specify deadband and the amount of stick-slip without the need for determining friction forces, the mass of the moving parts or the spring constant. Its behaviour matched closely to that of a first principles model.

Models for items of equipment such as motor drives, generators and turbines are well developed and commercially available in Simulink SimPower Systems from the Mathworks. The documentation gives an example of the use of a steam turbine model within an IEEE benchmark simulation [1] for a synchronous generator.

2.6. Models for teaching and training

Benchmark simulations have a role in teaching and several of those mentioned above feature in mainstream process control text books.

In the workplace, simulators are used to train process control operators especially in start-up and shut-down procedures and dealing with emergencies. Such simulators are specific for the process for which they were designed and generally include constraints and detailed representations of instruments, valves and equipment such as pumps. The Honeywell Shadow Plant simulator [13] is an example of a commercial training simulator.

2.7. Motivation for the CSTH simulation

The stirred tank heater model presented in this article is a hybrid simulation which uses measured data captured from a process to drive a first principles model. The noise and disturbances signals therefore have more complex and more realistic characteristics than if they were created by a random number generator. There are also experimentally measured data available for the purposes of identification.

It is a small model in comparison with many of those reviewed above, and there is no chemical reaction. It does, however have a complete characterization of all the sensors and valves and the heat exchanger. Its simplicity makes it primarily of value in a classroom setting, while the incorporation of constraints and non-linearities and the use of real noise sequences provide a practical benchmark for controller design and data-driven identification and diagnosis.

3. Process description and model

3.1. The continuous stirred tank heater

The pilot plant in the Department of Chemical and Materials Engineering at the University of Alberta is a stirred tank experimental rig in which hot and cold water are mixed, heated further using steam through a heating coil and drained from the tank through a long pipe. The configuration is shown in Fig. 1. The CSTH is well mixed and therefore the temperature in the tank is assumed the same as the outflow temperature. The tank has a circular cross section with a volume of 8 l and height of 50 cm.

3.2. Utilities and instrumentation

The utilities of the CSTH are shared services and therefore subject to disturbances from other users. The cold and hot water (CW and HW) in the building are pressurised with a pump to 60–80 psi, and the hot water boiler is heated by the university campus steam supply. The steam to the plant comes from the same central campus source.

Control valves in the CSTH plant have pneumatic actuators using 3–15 psi compressed air supply, the seat and stem sets being chosen to suit the range of control.

Flow instruments are orifice plates with differential pressure transmitters giving a nominal 4–20 mA output. The level instrument is also a differential pressure measurement. Finally, the temperature instrument is a type J metal sheathed thermocouple inserted into the outflow pipe with a Swagelock T-fitting.

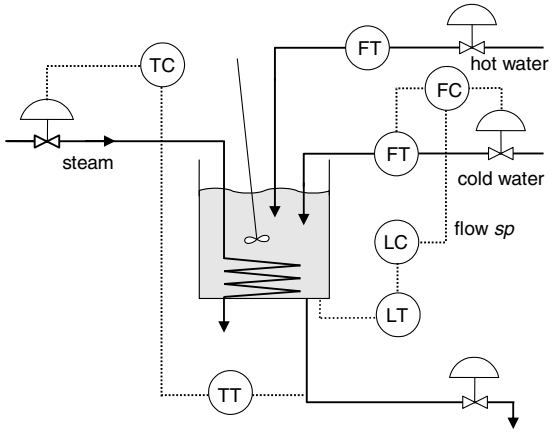

Fig. 1. The continuous stirred tank heater.

3.3. Volumetric and heat balance

The dynamic volumetric and heat balances are shown in the following equation:

$$\frac{dV(x)}{dt} = f_{cw} + f_{hw} - f_{out}(x) \quad (1)$$

$$\frac{dH}{dt} = W_{st} + h_{hw}\rho_{hw}f_{hw} + h_{cw}\rho_{cw}f_{cw} - h_{out}\rho_{out}f_{out}(x) \quad (2)$$

where x is the level; V the volume of water; f_{hw} the hot water flow into the tank; f_{cw} the cold water flow into the tank; f_{out} the outflow from tank; H the total enthalpy in the tank; h_{hw} the specific enthalpy of hot water feed; h_{cw} the specific enthalpy of cold water feed; h_{out} the specific enthalpy of water leaving the tank; ρ_{cw} the density of incoming cold water; ρ_{hw} the density of incoming hot water; ρ_{out} the density of water leaving the tank; and W_{st} the heat inflow from steam.

The temperatures of the hot and cold water feeds were set to 50 °C and 24 °C respectively in the base case simulation.

3.4. Related equations

The following algebraic equations also apply.

3.4.1. Specific enthalpy

In the well mixed case:

$$h_{out} = \frac{H}{V\rho_{out}} \quad (3)$$

3.4.2. Level, x

The relationship between level and volume is not linear because of the volume occupied by heating coils in the lower half of the tank. The relationship between level and volume was measured experimentally, as discussed in Section 3.5.

3.4.3. Outflow

The manual outflow valve was fixed at 50% as a standard operating condition. At this fixed setting, the empirical expression below was derived experimentally by seeking a square root relationship between the head of water in cm above the manual outflow valve and the measured flow in $m^3\ s^{-1}$.

$$f_{out} = 10^{-4}\left(0.1013 \times \sqrt{(55 + x)} + 0.0237\right)$$

The expression has this particular form because the manual outflow valve is 55 cm below the bottom of the tank and the head of water therefore is $55 + x$ where x is the level in the tank in cm.

3.4.4. Thermodynamic properties

The relationships between specific enthalpy, density and temperature in liquid water were taken from steam tables and used for the conversions of h to T, T to h, and T to ρ in piecewise linear look-up tables. Specific enthalpies are referenced to 0 °C.

3.4.5. Heat transfer from steam system

The heat transfer from the steam system depends on the steam valve setting. The relationship was determined empirically from steady state running at different steam valve settings since the heat exchange area and heat transfer coefficient could not be measured. The heat balance when the CSTH is in a steady state running with a cold water inflow only is:

$$W_{st} = h_{out}\rho_{out}f_{out} - h_{cw}\rho_{cw}f_{cw}$$

and $f_{cw} = f_{out}$ in steady state.

The calculations for W_{st} are in Table 1. The steady state flow in these experiments was 9.04 $10^{-5}\ m^3\ s^{-1}$, the incoming cold water temperature was 24 °C with $h_{cw} = 100.6\ kJ\ kg^{-1}$ and $\rho_{cw} = 997.1\ kg\ m^{-3}$.

The results of the calculations are used in a piecewise-linear look-up table that determines the amount of steam heating for a given steam valve setting. The data in Table 1 may be used in simulation under non-steady conditions given some assumptions:

(i) That the tank is well mixed so the temperature of the outflow is the same as that in the tank. The assumption is reasonable, because stirrer provides a high liquid velocity across the heating coils and distributes heat quickly throughout the tank.
(ii) That the amount of heat transferred at a given steam valve setting is not dependent on the temperature of the water in the tank. The assumption is reasonable since most of the heat in the steam is its latent heat of 2257 $kJ\ kg^{-1}$ compared to, say, the difference of 62.7 $kJ\ kg^{-1}$ between water at 25 °C and 40 °C.
(iii) That all the steam condenses and that circumstances do not arise where steam goes to waste. This assumption is reasonable unless the level is very low so that the heating coils are significantly exposed. It was observed that the maximum achievable temperature at the standard operating conditions was 65 °C when the steam valve was fully open. The steam should condense fully under these conditions.

3.5. Sensor and valve calibration

The inputs to the CSTH are electronic signals in the range 4–20 mA that go to the steam and cold water valves. The outputs are measurements from the temperature, level

Table 1
Relationship between heat transfer rate and steam valve setting

Valve/mA	T/°C	h_{out}/kJ kg^{-1}	ρ_{out}/kg m^{-3}	W_{st}/kJ s^{-1}
4	24	100.6	997.1	0
7.5	30	125.7	995.2	2.24
9	31	129.9	994.8	2.61
11	36.5	152.8	992.9	4.65
14	48	200.9	988.7	8.89
17	61	255.3	982.3	13.60
20	65	272.0	980.2	15.04

and cold water flow instruments, nominally in the range 4–20 mA. Calibration models were determined by measurement at several points in the range, and are represented in the model as piece-wise linear look-up tables. The level of detail presented in this section was found necessary to provide a high fidelity match between experimental observations and the simulation.

3.5.1. Level and volume

Data for the calibration of level and volume are plotted in Fig. 2a and b. The level instrument calibration converts the level in the tank to an instrument output on a 4–20 mA scale while the volume calibration gives a look-up table converting level in the tank to volume. The steam heating coils occupied a noticeable volume in the lower half of the tank and became fully covered when the level was 16.9 cm. Therefore the volume versus level characteristic is not linear when the level is low.

3.5.2. Cold and hot water flow calibration

Calibration of the cold and hot water valves is shown in Fig. 2c and d in which the volumetric flow rate is

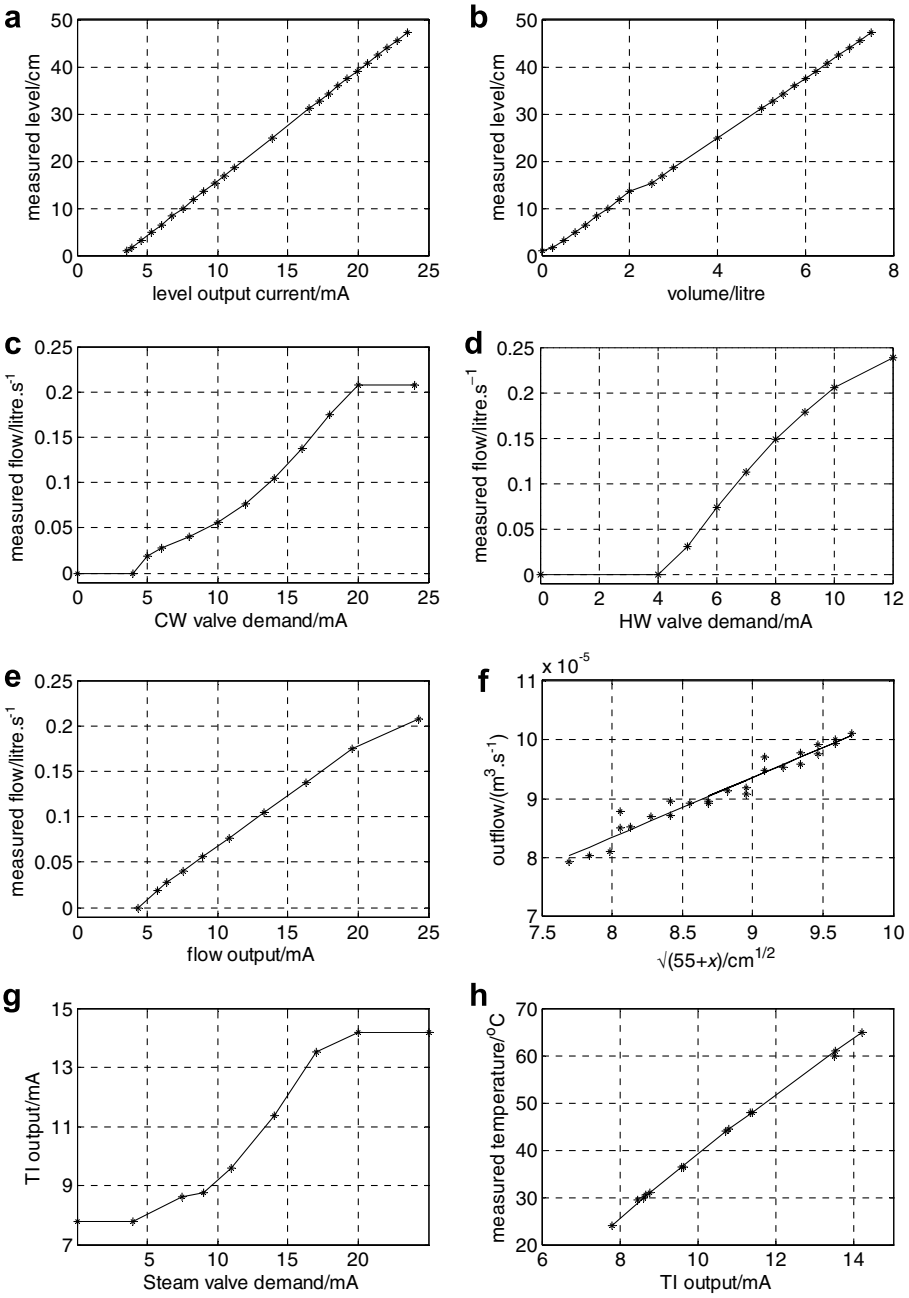

Fig. 2. Calibration graphs. (a) output of the level instrument and measured level, (b) measured volume and measured level, (c) cold water valve demand and measured cold water flow, (d) hot water valve demand and measured hot water flow, (e) cold water flow instrument output and measured cold water flow, (f) calibration of the outflow, (g) steam valve demand and thermocouple output and (h) thermocouple output and temperature measured with a thermometer.

plotted against the signal to the valve (valve demand). The CW valve becomes fully open when the demand signal is 20 mA and is fully shut at 4 mA. The flow rate was calculated by observation of the time taken to fill the tank with a known volume of water when the outflow valve was fully shut. The hot water valve is oversized and calibration beyond 12 mA was not possible because of splashing and the possibility of the tank overflowing.

Calibration of the cold water flow instrument is presented in Fig. 2e. It is almost linear over the 4–20 mA range of the instrument but the maximum cold water flow rate when the valve is fully open gives a measurement beyond the end of 4–20 mA scale. This calibration error has been reproduced in the CSTH simulation.

3.5.3. Outflow

Section 3.4 stated the relationship between the level in the tank and the flow through the outlet pipe as having the form:

$$f_{\text{out}} = m\sqrt{(55+x)} + c$$

The parameters m and c in the above expression were determined from the slope and vertical axis intercept of the best fit straight line to the graph in Fig. 2f which shows f_{out} plotted against the constructed quantity $\sqrt{(55+x)}$, where x is the level of water in the tank in cm. The experimental procedure used closed loop control of level. The steady state inflow that balanced the outflow at each level set point was determined from the cold water flow instrument and converted to engineering units via Fig. 2e. Each level set point gave one plotted point in Fig. 2f. The measured flow was variable during each experiment because of a disturbance to the cold water flow (to be discussed in Section 6). It also was not fully reproducible between experiments, possibly because the flow regime in the outflow tube is turbulent.

3.5.4. Temperature calibration

Fig. 2g shows outputs of the thermocouple for various steady state steam valve demand settings, while Fig. 2h shows an almost linear relationship between thermocouple output and temperature in the tank measured with a mercury thermometer.

3.5.5. Cold water valve model

From step testing, the cold water valve dynamics were found to be those of a first order lag with time delay. The time delay is 1 s and the time constant of the valve is 3.8 s. Thus the valve transfer function is:

$$MV(s) = \frac{e^{-s}}{3.8s+1} OP(s) \tag{4}$$

where $MV(s)$ represents the valve position. In closed loop, $OP(s)$ is the controller output while in open loop it is a valve demand signal applied directly to the valve.

4. Simulation

4.1. The Simulink platform

An equation-based simulator is needed for numerical solution of the CSTH model equations and in this article the simulation was carried out in Simulink. This section gives some details of the implementation. Simulink is a sequential solver, and therefore it is necessary to specify which variables are independent inputs into the equations and which are dependent outputs that will be calculated during the simulation.

4.2. Inputs and outputs

As in the real plant, the simulation inputs and outputs represent electronic signals on 4–20 mA scale. The inputs are the CW, HW and steam valve demands. Outputs are the electronic measurements from the level, cold and hot water flow and temperature instruments. The aim of simulation is to determine the dynamic responses of the outputs for specified time-varying or steady inputs.

Look-up tables derived from Fig. 2c and d convert the 4–20 mA CW and HW valve demand to f_{cw} and f_{hw} values in $\text{m}^3\,\text{s}^{-1}$ and the steam valve demand is converted to a steam enthalpy flow rate in $\text{kJ}\,\text{s}^{-1}$. At the output, the calibration look-up tables convert level, water flow rates and temperature to 4–20 mA values.

4.3. Heat and volumetric balances

The volumetric balance transforms the current value of the cold water inflow into volume, level and outflow by integration of Eq. (1). The volume and outflow become inputs to the heat balance model along with the steam valve setting and cold water inflow. The heat balance model integrates Eq. (2) while the temperature is determined from the algebraic relationship in (3) together with a piece-wise linear look-up table for the thermodynamic properties of water.

4.4. Controllers

The control system is not part of the CSTH model. It is straightforward to construct closed loop control of the implemented Simulink model using the inputs and outputs provided.

4.4.1. Controller formulation

The standard form in process control for a proportional plus integral controller is

$$C(s) = K_{\text{c}}\left(1 + \frac{1}{\tau_{\text{i}} s}\right)$$

where K_{c} is the controller gain and τ_{i} is the integration time. The PI controller provided by Simulink, by contrast,

requires specification of the control and integrator gain, as follows:

$$C(s) = P + \frac{I}{s}$$

where $P = K_c$ and $I = K_c/\tau_i$. A consequence of the Simulink form is that both P and I must change in proportion if the controller gain K_c is adjusted.

5. Model validation

This section presents a comparison between simulation and experimental results in open and closed loop.

5.1. Open loop testing

Open loop testing involved steps in the positions of the cold water flow and steam valves and observation of the cold water flow rate and temperature. For the temperature tests, the level was held constant at a set point of 12 mA (20.48 cm). The results are shown in Fig. 3 where it can be seen that the steady state gains and the dynamics of the transients are generally simulated accurately especially in the middle of the operating range. The lower left panel of Fig. 3 suggests the steam valve sometimes behaves differently when closing, an effect that has not been captured by the simulation.

5.2. Closed loop testing

Closed loop tests were made on the temperature and level control loops at different controller settings. The P and I values were chosen to span the range from sluggish to overly tight control. Figs. 4 and 5 show the match between simulation and experiment is generally acceptable giving confidence that the simulation can act as a reliable proxy for the physical CSTH plant.

6. Disturbances

Disturbances to the experimental pilot plant comprise a deterministic oscillatory disturbance to the cold water flow rate, a random disturbance to the level, and temperature measurement noise. The strategy used for preparation of the benchmark simulation was to capture data from the experimental pilot plant and to feed those data into the simulation from data files in order to provide realistic disturbances.

6.1. Cold water flow disturbance

The cold water flow in the experimental plant had a deterministic oscillatory disturbance with a period of about 40 s that originated elsewhere in the building. This disturbance was captured by measuring the cold water flow through the valve with the cold water valve open at its mid-point on the 4–20 mA scale. The outlet valve of the tank was opened fully during the experiment, therefore the tank ran empty. A portion of the disturbance is shown in the top panel of Fig. 6 where its oscillatory nature can be seen.

6.2. Level disturbance caused by bubbles

The experimental plant has the facility to blow compressed air into the tank. The compressed air causes bubbles which disturb the level in the tank. The bubble disturbance

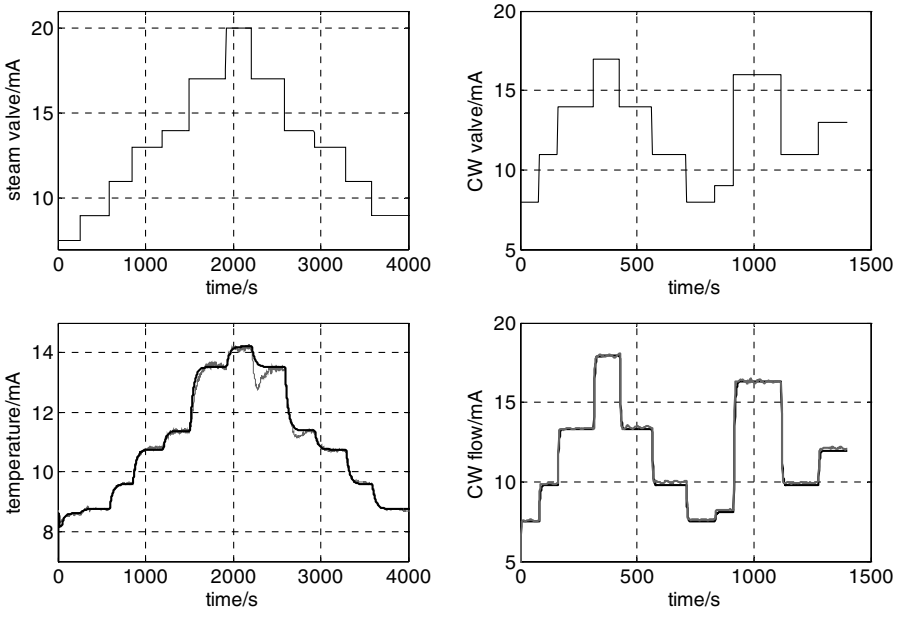

Fig. 3. Open loop tests. Left hand panels: temperature steps, Right hand panels: steps in the cold water flow. Black lines are the simulation, grey lines are experimental results.

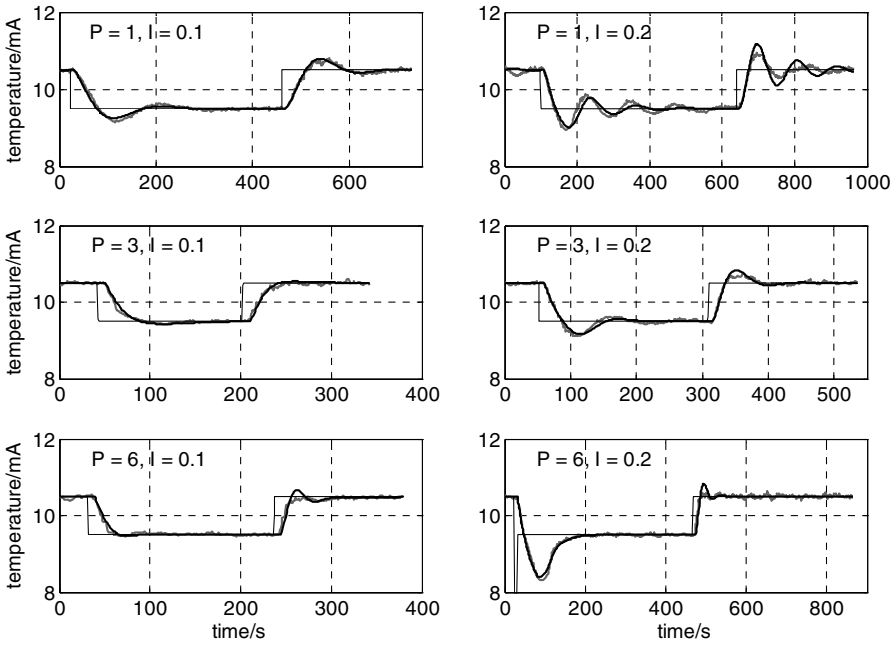

Fig. 4. Comparison of closed loop step tests in the temperature loop, simulation and experiment. Black lines are the simulation, grey lines are experimental results.

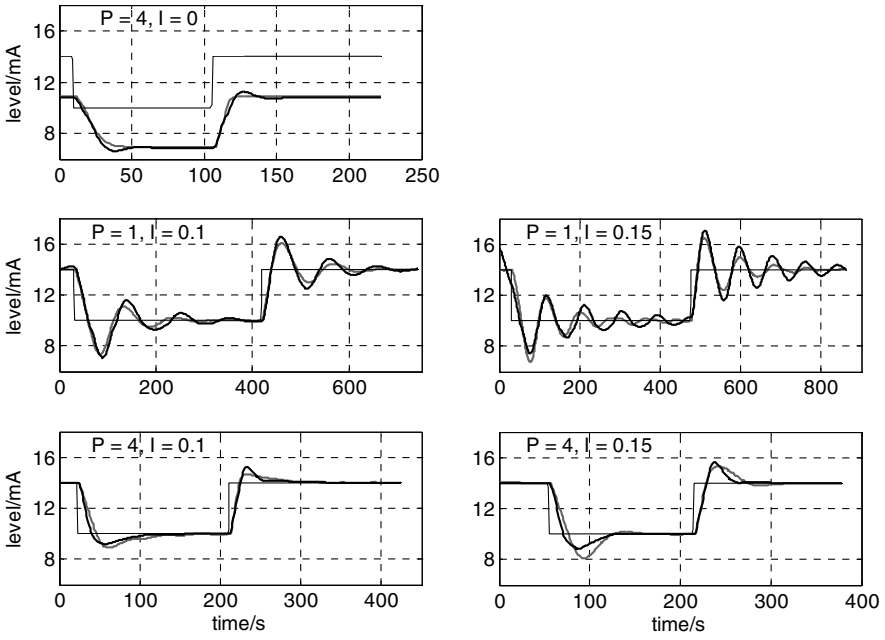

Fig. 5. Comparison of closed loop step tests in the level loop, simulation and experiment. Black lines are the simulation, grey lines are experimental results.

was monitored as the output from the level instrument with the tank half full and with the inlet and outlet valves both closed. The nature of the disturbance is random.

6.3. Temperature measurement noise

The temperature measurement noise was monitored with the tank half full and under closed loop level and temperature control. It has high frequency components and some medium term lower frequency fluctuations can also be seen.

6.4. Simulation with disturbances

The disturbances can be added to the simulation as follows:

- The cold water flow disturbance d_{cw} in mA is added to the cold water valve position to give $mv_d(t) = mv(t) + d_{cw}$, where mv is the time domain output of the valve transfer function (4).
- The level disturbance in mA is converted to a disturbance in volume d_V by means of an algebraic

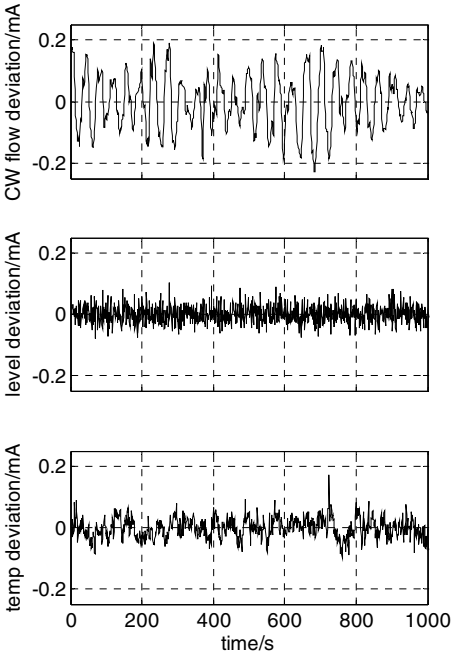

Fig. 6. Upper panel: CW flow disturbance, Middle: level disturbance due to bubbles, Bottom: temperature measurement noise.

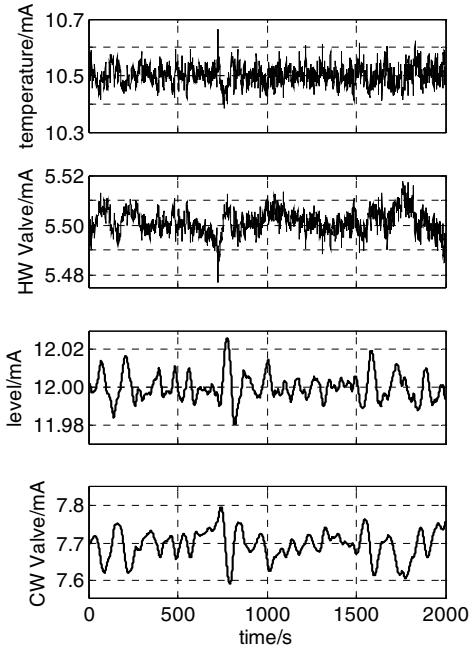

Fig. 7. Simulated demonstration of a controller interaction in which temperature noise upsets level and cold water flow.

relationship based on Fig. 2a and b. It is added to output of integration of the volumetric balance Eq. (1). Hence the equations for the disturbed level x_d become:

$$\frac{dV}{dt} = f_{cw} + f_{hw} - f_{out}$$
$$x_d(t) = x(V(t) + d_V)$$

- The temperature noise is converted first to d_T, a temperature deviation in °C using the algebraic relationship in Fig. 2h. It is added to the temperature calculated from the heat balance to give a noisy temperature measurement T_d. The necessary steps are numerical integration to determine H and the conversion of H to T by means of Eq. (3) and a look-up table for the thermodynamic properties of water.

$$\frac{dH}{dt} = W_{st} + h_{hw}\rho_{hw}f_{hw} + h_{cw}\rho_{cw}f_{cw} - h_{out}\rho_{out}f_{out}$$
$$T_d(t) = T(H(t)) + d_T(t)$$

6.5. Example of simulation with a disturbance

An advantage of a simulation with noise or a disturbance is that the disturbance can excite and drive dynamic effects in other parts of the model. An example is shown which demonstrates a controller interaction when the temperature is controlled via the hot water inflow rather than via steam heating. An interaction arises between the level control loop and the hot water flow loop because the action of the hot water temperature control affects the level.

Fig. 7 shows the behaviour of the closed loop simulation when temperature noise is present. The temperature noise leads to persistent activity of the hot water flow valve via the temperature control loop, which upsets the level. The lower two panels show that the dynamics of the closed loop level control system filter the disturbance and amplify some frequencies relative to others to give a smooth and rather oscillatory disturbance in the cold water valve position and level.

7. Linearization

7.1. Standard operating conditions

Many simulation examples from the literature are presented in the form of a state-space model or as a matrix of transfer functions. These forms are also presented here to make the stirred tank heater model accessible for linear multivariable control design and analysis. Two operating points have been linearized, one with the stirred tank

Table 2
Operating points for linearization

Variable	Op Pt 1	Op Pt 2
Level/mA	12.00	12.00
Level/cm	20.48	20.48
CW flow/mA	11.89	7.330
CW flow/$m^3\ s^{-1}$	9.038×10^{-5}	3.823×10^{-5}
CW valve/mA	12.96	7.704
Temperature/mA	10.50	10.50
Temperature/°C	42.52	42.52
Steam valve/mA	12.57	6.053
HW valve/mA	0	5.500
HW flow/$m^3\ s^{-1}$	0	5.215×10^{-5}

heater operating with only a cold water feed and the other with both hot and cold water feed.

The steady state valve positions and instrument conditions in each case are shown in Table 2. Variables in the linearized models are deviations from the operating point. Time delays are present at the input and output. The CW valve has a time delay of 1 s while the temperature measurement delay is 8 s.

7.2. Operating point 1

7.2.1. Open loop state-space model

The state-space model is

$$\frac{d\underline{\mathbf{x}}}{dt} = \mathbf{A}\underline{\mathbf{x}} + \mathbf{B}\underline{\mathbf{u}}'$$
$$\underline{\mathbf{y}}' = \mathbf{C}\underline{\mathbf{x}}$$
$$\begin{pmatrix} u_1'(t) \\ u_2'(t) \end{pmatrix} = \begin{pmatrix} u_1(t-1) \\ u_2(t) \end{pmatrix} \quad \text{and} \quad \begin{pmatrix} y_1(t) \\ y_2(t) \\ y_3(t) \end{pmatrix} = \begin{pmatrix} y_1'(t) \\ y_2'(t) \\ y_2'(t-8) \end{pmatrix}$$

where u_1 is the cold water valve position in mA; u_2 the steam valve position in mA; y_1 the level measurement in mA; y_2 the cold water flow measurement in mA; y_3 the temperature measurement in mA; x_1 the tank volume, output of the integrator in Eq. (1); x_2 the output of the integrator in the valve transfer function in Eq. (4); x_3 the total enthalpy in the tank, output of the enthalpy integrator in Eq. (2).

$$\mathbf{A} = \begin{pmatrix} -3.7313 \times 10^{-3} & 3.6842 \times 10^{-6} & 0 \\ 0 & -2.6316 \times 10^{-1} & 0 \\ 4.1580 \times 10^{3} & 3.6964 \times 10^{-1} & -2.7316 \times 10^{-2} \end{pmatrix}$$
$$\mathbf{B} = \begin{pmatrix} 0 & 0 \\ 1 & 0 \\ 0 & 1.4133 \end{pmatrix}$$
$$\mathbf{C} = \begin{pmatrix} 2690.0 & 0 & 0 \\ 0 & 2.8421 \times 10^{-1} & 0 \\ -1979.2 & 0 & 1.1226 \times 10^{-2} \end{pmatrix}$$

7.2.2. Open loop transfer function model

The transfer function model has the following form where $\mathbf{U}(s)$ and $\mathbf{Y}(s)$ are the Laplace transforms of the vectors of input and output variables.

$$\mathbf{Y}(s) = \mathbf{G}(s)\mathbf{U}(s) = \begin{pmatrix} G_{11}(s) & 0 \\ G_{21}(s) & 0 \\ G_{31}(s) & G_{32}(s) \end{pmatrix} \mathbf{U}(s)$$

where

$$G_{11}(s) = \frac{9.9105 \times 10^{-3} e^{-s}}{(s + 3.731 \times 10^{-3})(s + 2.632 \times 10^{-1})}$$
$$G_{21}(s) = \frac{2.8421 \times 10^{-1} e^{-s}}{(s + 2.632 \times 10^{-1})}$$
$$G_{31}(s) = \frac{-3.1422 \times 10^{-3} e^{-9s}}{(s + 2.732 \times 10^{-2})(s + 2.632 \times 10^{-1})}$$
$$G_{32}(s) = \frac{1.5867 \times 10^{-2} e^{-8s}}{(s + 2.732 \times 10^{-2})}$$

7.3. Operating point 2

7.3.1. Open loop state-space model

The state-space model is

$$\frac{d\underline{\mathbf{x}}}{dt} = \mathbf{A}\underline{\mathbf{x}} + \mathbf{B}\underline{\mathbf{u}}'$$
$$\underline{\mathbf{y}}' = \mathbf{C}\underline{\mathbf{x}}$$
$$\begin{pmatrix} u_1'(t) \\ u_2'(t) \\ u_3'(t) \end{pmatrix} = \begin{pmatrix} u_1(t-1) \\ u_2(t) \\ u_3(t) \end{pmatrix} \quad \text{and} \quad \begin{pmatrix} y_1(t) \\ y_2(t) \\ y_3(t) \end{pmatrix} = \begin{pmatrix} y_1'(t) \\ y_2'(t) \\ y_2'(t-8) \end{pmatrix}$$

where u_1 is the cold water valve position in mA; u_2 the steam valve position in mA; u_3 the hot water valve position in mA; y_1 the level measurement in mA; y_2 the cold water flow measurement in mA; y_3 temperature measurement in mA; x_1 the tank volume, output of the integrator in Eq. (1); x_2 the output of the integrator in the valve transfer function in Eq. (4) and x_3 the total enthalpy in the tank, output of the enthalpy integrator in Eq. (2).

$$\mathbf{A} = \begin{pmatrix} -3.7313 \times 10^{-3} & 1.5789 \times 10^{-6} & 0 \\ 0 & -2.6316 \times 10^{-1} & 0 \\ 4.1580 \times 10^{3} & 1.5842 \times 10^{-1} & -2.7316 \times 10^{-2} \end{pmatrix}$$
$$\mathbf{B} = \begin{pmatrix} 0 & 0 & 4.2900 \times 10^{-5} \\ 1 & 0 & 0 \\ 0 & 6.4000 \times 10^{-1} & 8.8712 \end{pmatrix}$$
$$\mathbf{C} = \begin{pmatrix} 2690.0 & 0 & 0 \\ 0 & 1.5132 \times 10^{-1} & 0 \\ -1979.2 & 0 & 1.1226 \times 10^{-2} \end{pmatrix}$$

7.3.2. Open loop transfer function model

$$\mathbf{Y}(s) = \mathbf{G}(s)\mathbf{U}(s) = \begin{pmatrix} G_{11}(s) & 0 & G_{13}(s) \\ G_{21}(s) & 0 & 0 \\ G_{31}(s) & G_{32}(s) & G_{33}(s) \end{pmatrix} \mathbf{U}(s)$$

where

$$G_{11}(s) = \frac{4.2474 \times 10^{-3} e^{-s}}{(s + 3.731 \times 10^{-3})(s + 2.632 \times 10^{-1})}$$
$$G_{21}(s) = \frac{1.5132 \times 10^{-1} e^{-s}}{(s + 2.632 \times 10^{-1})}$$
$$G_{31}(s) = \frac{-3.1466 \times 10^{-3} e^{-9s}}{(s + 2.732 \times 10^{-2})(s + 2.632 \times 10^{-1})}$$
$$G_{32}(s) = \frac{7.1849 \times 10^{-3} e^{-8s}}{(s + 2.732 \times 10^{-2})}$$
$$G_{13}(s) = \frac{1.1540 \times 10^{-1}}{(s + 3.731 \times 10^{-3})}$$
$$G_{33}(s) = \frac{1.4683 \times 10^{-2} e^{-8s}}{(s + 2.732 \times 10^{-2})}$$

8. Example applications

8.1. Suggested applications

There are several possible educational and academic applications for a benchmark simulation that has accurate measurement of non-linearities and constraints, real noise sequences captured from the plant, and full experimental validation. Suggested uses include:

- a teaching resource for a control systems course;
- generation of realistic data for testing of data-driven methods;
- testing of fault detection and diagnosis algorithms;
- in conjunction with a valve model [6], generation of realistic data for valve fault diagnosis;
- exploration of new or modified control algorithms that are robust to windup, non-linearity and model-mismatch.

8.2. System identification task

This section gives an illustration of the use of the CSTH simulation in a system identification experiment. The data are presented and a challenge laid down to identify the linearized dynamics.

8.2.1. Closed loop system identification

Simulation and experimental runs from a system identification experiment were carried out. The aim is to identify the two-by-two system with level and temperature as measured outputs and level loop setpoint and temperature

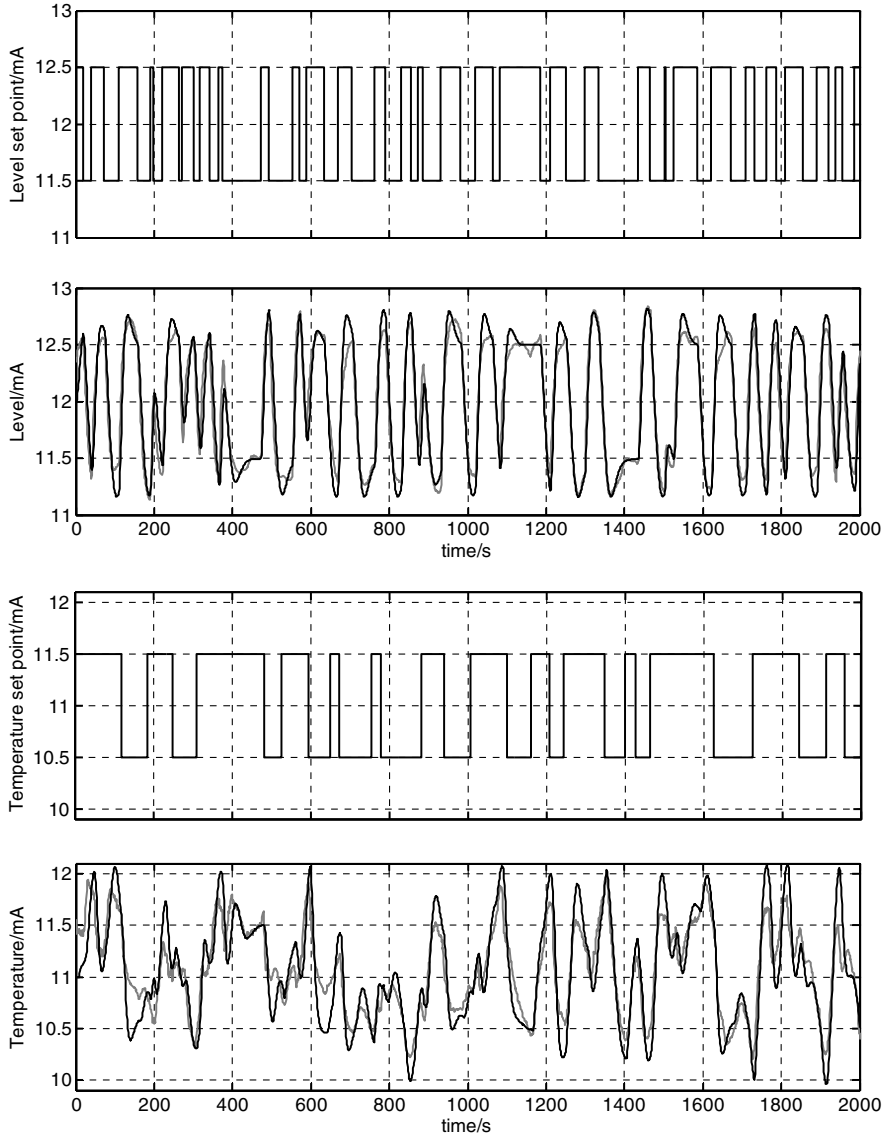

Fig. 8. System identification. Upper panels: Level set point and measurement, Lower panels: Temperature set point and measurement. Black lines are the simulation, grey lines are experimental results.

loop setpoint as manipulated inputs. The level and the temperature setpoints were simultaneously perturbed with random binary inputs of amplitude 0.5 mA and 1 mA respectively generated using the *idinput* function in System Identification Toolbox of MATLAB. The level and temperature variations are presented in Fig. 8 which shows the simulation generally matches the experimental results well. The match suggests the simulation can provide a resource for the investigation of new system identification methods.

The data and a simulation for system identification are provided at the simulation web site. As well as providing the random binary inputs, it allows the additional disturbances from Fig. 6 to be activated to test the robustness of the system identification methods.

Linearization of the closed loop model gives the transfer function presented below. The CW valve and temperature instrument time delays cannot be referred to the input and output in this example because the level and temperature are under closed loop control. They are handled as first order Padé approximations giving rise to right half plane zeros in the linearized transfer functions.

The task is to use the simulated data of Fig. 8 (available at the CSTH web site) to identify transfer functions which closely match those derived from direct linearization of the model.

8.2.2. Transfer function model from direct linearization

$$\mathbf{G}(\mathrm{s}) = \begin{pmatrix} G_{11}(s) & G_{12}(s) \\ 0 & G_{22}(s) \end{pmatrix}$$

where

$$G_{11}(s) = \frac{-0.029732(s-2)(s+0.0375)}{(s+2.033)(s+0.05799)(s^2+0.1881s+0.01139)}$$

$$G_{12}(s) = \frac{0.013915s(s-2)(s-4)(s-0.2667)}{(s+3.931)(s+2.033)(s+0.05799)(s+0.04015)} \times \frac{(s+0.0375)(s+0.003731)}{(s^2+0.1881s+0.01139)(s^2+0.1761s+0.01892)}$$

$$G_{22}(s) = \frac{0.050561(s-4)(s-0.2667)(s+0.03333)}{(s+3.931)(s+0.04015)(s^2+0.1881s+0.01139)} \quad (5)$$

9. Summary and concluding remarks

A simulation of a continuous stirred tank heater at the University of Alberta has been presented, and a Simulink implementation used to generate results in open and closed loop. Instrument, actuator and process non-linearities have been characterized and the simulation has a hybrid nature because real process and measurement noise sequences are used as disturbances. Linearized state-space and transfer function models are also provided for the purposes of linear multivariable controller design and other activities where linear approximations are utilized.

The Simulink model and experimental data are available electronically, and a some suggestions are given for applications including a system identification task.

Acknowledgements

The authors thank Mr Walter Boddez, Instrument Shop Supervisor in the Department of Chemical and Materials Engineering, University of Alberta, for technical inputs and insights about the CSTH equipment. The first author gratefully acknowledges the support of the Royal Academy of Engineering (Foresight Award). The authors are grateful for the support of the Natural Science and Engineering Research Council (Canada), Matrikon (Edmonton, Alberta) and the Alberta Science and Research Authority through the NSERC-Matrikon-ASRA Industrial Research Chair in Process Control. The authors thank the editors for the opportunity to prepare a paper for this Special Issue of the Journal of Process Control, and we offer Dale the most sincere congratulations and best wishes on the occasion of his 65th birthday.

Appendix A1. The CSTH web site

A web page has been prepared to house the CSTH simulation models and data. Its location is: http://www.ps.ic.ac.uk/~nina/CSTHSimulation/index.htm. The contents include

- A general purpose Simulink model with level and temperature control loops;
- A general purpose Simulink model with level and temperature control loops and disturbances;
- Open loop Simulink models for the operating points in Table 2, together with MATLAB code to organize the linearization;
- A Simulink model with level and temperature control loops for the system identification task of Section 8.2;
- Data files for the disturbance sequences in Fig. 6;
- Data files for the input sequences in Fig. 8.

Additional materials are also available. These are (i) a set of data for fault identification, (ii) a simulation of a modified continuous stirred tank heater from the laboratory of Professor Patwardhan at IIT Bombay, as described briefly in Appendix A2. This CSTH system has a recycle and shows non-minimum phase behaviour at some operating points.

Appendix A2. A modified CSTH model

A modified CSTH has been developed in the Automation Laboratory at Department of Chemical Engineering, IIT Bombay. The reason for presenting the modified CSTH here is that a simulation is provided at the CSTH web site.

This system consists of an additional stirred tank upstream of the CSTH (Fig. 9). The cold water entering

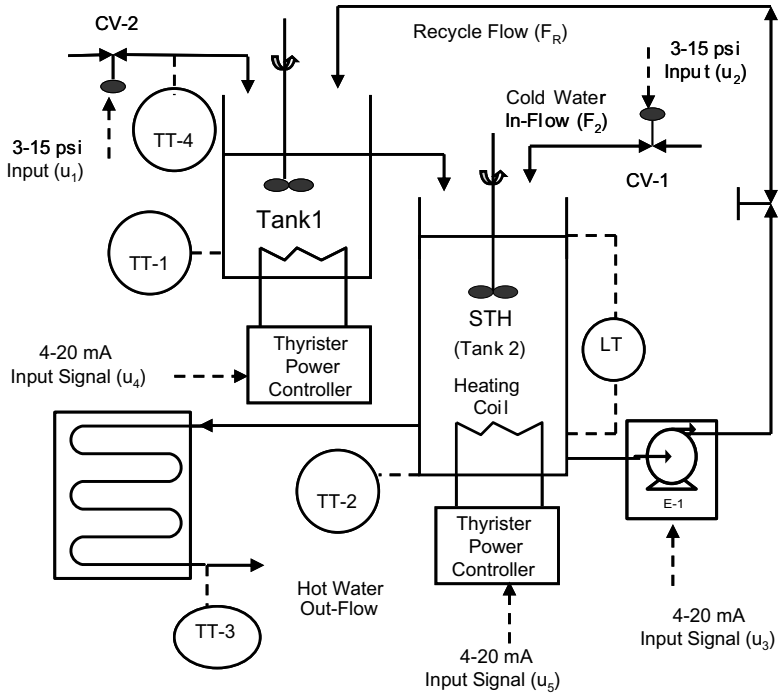

Fig. 9. Modified CSTH system in IIT Bombay.

Tank 1 and Tank 2 is heated using two separate electrical heaters. A portion of hot water from Tank 2 is recycled to Tank 1, which introduces additional multivariable interactions and additional complexity in the system, including an inverse response at some operating points.

A grey-box model has been developed for the modified STH system as follows

$$V_1\frac{dT_1}{dt} = F_1(u_1)(T_c - T_1) + F_R(u_3)(T_2 - T_1) + \frac{Q_1(u_4)}{\rho C_p}$$

$$A_2h_2\frac{dT_2}{dt} = F_1(u_1)(T_1 - T_2) + F_2(u_2)(T_c - T_2) - F_R(u_3) \times (T_2 - T_1) + \frac{1}{\rho C_p}[Q_2(u_5) - 2\pi r_2h_2U(T_2 - T_a)]$$

$$A_2\frac{dh_2}{dt} = F_1(u_1) + F_2(u_2) - F_{out}(h_2)$$

$$F_{out}(h_2) = 0.1 \times 10^{-3} \times \sqrt{(0.406h_2^3 + 0.8061h_2^2 - 0.01798h_2 + 0.1054)} \quad (6)$$

The flow rates are functions of inputs u_1, u_2 and u_3 as given by the following correlations, where the flow rates are in $m^3\ s^{-1}$:

$$F_1(u_1) = (42379u_1 - 456.85u_1^2 + 8.0368u_1^3) \times 10^{-11}$$

$$F_2(u_2) = (196620u_2 - 8796.8u_2^2 + 190.64u_2^3 - 1.294u_2^4) \times 10^{-11}$$

$$F_R(u_3) = 2u_3 \times (1/3600) \times 10^{-3}$$

Also, the heat inputs are functions of inputs u_4 and u_5 as given by following correlations, where the heat flows Q_1 and Q_2 are in $J\ s^{-1}$:

$$Q_1(u_4) = 7.9798u_4 + 0.9893u_4^2 - 7.3 \times 10^{-3}u_4^3$$

$$Q_2(u_5) = 104 + 14.44u_5 + 0.96u_5^2 - 8 \times 10^{-3}u_5^3$$

It may be noted that inputs $u_1, \ldots, u_5$ in all the correlations stated above are expressed in terms of % values between 0 and 100%. The model parameters and steady states are listed in Table 3.

Table 3
Nominal model parameters and steady state

Parameter	Description	Value
V_1	Volume of tank 1	1.75×10^{-3} m^3
A_2	Cross sectional area of tank 2	7.854×10^{-3} m^2
r_2	Radius of tank 2	0.05 m
U	Heat transfer coefficient	235.1 W/m^2 K
T_c	Cooling water temperature	30 °C
T_a	Atmospheric temperature	25 °C
u_1	Flow F_1 (% Input)	60%
u_2	Flow F_2 (% Input)	55%
u_3	Flow F_R (% Input)	50%
u_4	Heat input Q_1 (% Input)	60%
u_5	Heat input Q_2 (% Input)	80%
T_1	Steady state temperature (tank 1)	49.77 °C
T_2	Steady state temperature (tank 2)	52.92 °C
h_2	Steady state level	0.3599 m

References

[1] Anon, Second benchmark model for computer simulation of SSR, IEEE Transactions on Power Apparatus and Systems PAS-104 (1985) 1057–1066.

[2] M. Bartys, R. Patton, M. Syfert, S. de Las Heras, J. Quevedo, Introduction to the DAMADICS actuator FDI benchmark study, Control Engineering Practice 14 (2006) 577–596.

[3] D. Chen, D.E. Seborg, Relative gain array analysis for uncertain process models, AIChE Journal 48 (2002) 302–310.
[4] R. Chen, K. Dave, T.J. McAvoy, M. Luyben, A non-linear dynamic model of a vinyl acetate process, Industrial and Engineering Chemistry Research 42 (2003) 4478–4487.
[5] L.H. Chiang, E.L. Russell, R.D. Braatz, Fault diagnosis in chemical processes using Fisher discriminant analysis, discriminant partial least squares, and principal component analysis, Chemometrics and Intelligent Laboratory Systems 50 (2000) 243–252.
[6] M.A.A.S. Choudhury, N.F. Thornhill, S.L. Shah, Modelling valve stiction, Control Engineering Practice 13 (2005) 641–658.
[7] R. Dixon, A.W. Pike, Alstom benchmark challenge II on gasifier control, IEE Proceedings-Control Theory and Applications 153 (2006) 254–261.
[8] R. Dixon, A.W. Pike, M.S. Donne, The ALSTOM benchmark challenge on gasifier control, Proceedings of the Institution of Mechanical Engineers Part I-Journal of Systems and Control Engineering 214 (2000) 389–394.
[9] J.J. Downs, E.F. Vogel, A plant-wide industrial-process control problem, Computers and Chemical Engineering 17 (1993) 245–255.
[10] F.J. Doyle III, R.K. Pearson, B.A. Ogunnaike, Identification and Control Using Volterra Models, Springer, 2001, ISBN 978-1852331498.
[11] J. Gao, A. Penlidis, Mathematical modeling and computer simulator/database for emulsion polymerizations, Progress in Polymer Science 27 (2002) 403–535.
[12] J. Gertler, W.H. Li, Y.B. Huang, T. McAvoy, Isolation enhanced principal component analysis, AIChE Journal 45 (1999) 323–334.
[13] Honeywell, 2006, Shadow Plant System. On-line: http://hpsweb.honeywell.com/Cultures/en-US/Support/SystemProducts/Simulation/default.htm . Accessed 29th July 2007.
[14] B.C. Juricek, D.E. Seborg, W.E. Larimore, Identification of the Tennessee Eastman challenge process with subspace methods, Control Engineering Practice 9 (2001) 1337–1351.
[15] M. Kano, S. Hasebe, I. Hashimoto, H. Ohno, A new multivariate statistical process monitoring method using principal component analysis, Computers and Chemical Engineering 25 (2001) 1103–1113.
[16] M. Kano, K. Nagao, S. Hasebe, I. Hashimoto, H. Ohno, R. Strauss, B.R. Bakshi, Comparison of multivariate statistical monitoring methods with applications to the Eastman challenge problem, Computers and Chemical Engineering 26 (2002) 161–174.
[17] L.S. Kershenbaum, P. Kittisupakorn, The use of a partially simulated exothermic (PARSEX) reactor for experimental testing of control algorithms, Chemical Engineering Research and Design 72 (1994) 55–63.
[18] J. Korvink, 2004. Oberwolfach model reduction benchmark collection, On-line: http://www.imtek.de/simulation/index_en.php. Accessed 29th July 2007.
[19] W.F. Ku, R.H. Storer, C. Georgakis, Disturbance detection and isolation by dynamic principal component analysis, Chemometrics and Intelligent Laboratory Systems 30 (1995) 179–196.
[20] T. Larsson, K. Hestetun, E. Hovland, S. Skogestad, Self-optimizing control of a large-scale plant: The Tennessee Eastman process, Industrial and Engineering Chemistry Research 40 (2001) 4889–4901.
[21] F. Loquasto, D.E. Seborg, Monitoring model predictive control systems using pattern classification and neural networks, Industrial and Engineering Chemistry Research 42 (2003) 4689–4701.
[22] M.L. Luyben, B.D. Tyreus, W.L. Luyben, Plantwide control design procedure, AIChE Journal 43 (1997) 3161–3174.
[23] P.R. Lyman, C. Georgakis, Plant-wide control of the Tennessee Eastman problem, Computers and Chemical Engineering 19 (1995) 321–331.
[24] T.J. McAvoy, N. Ye, Base control for the Tennessee Eastman problem, Computers and Chemical Engineering 18 (1994) 383–413.
[25] R.C. McFarlane, R.C. Reineman, J.F. Bartee, C. Georgakis, Dynamic simulator for a model-IV fluid catalytic cracking unit, Computers and Chemical Engineering 17 (1993) 275–300.
[26] B.A. Ogunnaike, W.H. Ray, Process Dynamics, Modeling, and Control (Topics in Chemical Engineering), Oxford University Press, 1994.
[27] B.A. Ogunnaike, J. Lemaire, M. Morari, W.H. Ray, Advanced multivariable control of a pilot plant distillation column, AIChE Journal 29 (1983) 632–640.
[28] D. Prett, M. Morari, The Shell Process Control Workshop, Butterworths, Houston, London, TX, 1987, December 15–18.
[29] N.L. Ricker, Tennessee Eastman challenge archive, 1999, On-line: http://depts.washington.edu/control/LARRY/TE/download.html. Accessed 29th July 2007.
[30] N.L. Ricker, J.H. Lee, Non-linear model-predictive control of the Tennessee-Eastman challenge process, Computers and Chemical Engineering 19 (1995) 961–981.
[31] L.P. Russo, B.W. Bequette, Impact of process design on the multiplicity behavior of a jacketed exothermic CSTR, AIChE Journal 41 (1995) 135–147.
[32] L.P. Russo, B.W. Bequette, Effect of process design on the open-loop behavior of a jacketed exothermic CSTR, Computers and Chemical Engineering 20 (1996) 417–426.
[33] D.E. Seborg, T.E. Edgar, D.A. Mellichamp, Process Dynamics and Control, second ed., John Wiley, Hoboken, NJ, 2004.
[34] A. Singhal, D.E. Seborg, Evaluation of a pattern matching method for the Tennessee Eastman challenge process, Journal of Process Control 16 (2006) 601–613.
[35] S. Skogestad, M. Morari, Understanding the dynamic behavior of distillation columns, Industrial and Engineering Chemistry Research 27 (1988) 1848–1862.
[36] S. Skogestad, MATLAB Distillation column model (ColumnA), Online: http://www.nt.ntnu.no/users/skoge/book/matlab_m/cola/cola.html. Accessed 29th July 2007.
[37] SLICOT, 2005, The Control and Systems Library, On-line: http://www.slicot.de/index.php?site=benchmarks. Accessed 29th July 2007.
[38] N.F. Thornhill, S.C. Patwardhan, S.L. Shah, 2007, The CSTH simulation website, online: http://www.ps.ic.ac.uk/~nina/CSTHSimulation/index.htm. Accessed 29th July 2007.
[39] J.G. Van de Vusse, Plug-flow type reactor versus tank reactor, Chemical Engineering Science 19 (1964) 994–997.
[40] P. Wang, T. McAvoy, Synthesis of plantwide control systems using a dynamic model and optimization, Industrial and Engineering Chemistry Research 40 (2001) 5732–5742.
[41] B.M. Wise, D. Haesloop, A non-linear dynamic model identification challenge problem, Chemometrics and Intelligent Laboratory Systems 30 (1995) 91–96.
[42] R.K. Wood, M.W. Berry, Terminal composition control of a binary distillation column, Chemical Engineering Science 28 (1973) 1707–1717.